We are IntechOpen, the world's leading publisher of Open Access books
Built by scientists, for scientists

4,800
Open access books available

122,000
International authors and editors

135M
Downloads

Our authors are among the

154
Countries delivered to

TOP 1%
most cited scientists

12.2%
Contributors from top 500 universities

CLARIVATE ANALYTICS
BOOK CITATION INDEX
INDEXED

WEB OF SCIENCE™

Selection of our books indexed in the Book Citation Index in Web of Science™ Core Collection (BKCI)

Interested in publishing with us?
Contact book.department@intechopen.com

Numbers displayed above are based on latest data collected.
For more information visit www.intechopen.com

Chapter

Evolution of Nanometer-to-Micrometer Grain Size in Multiferroic Properties of Polycrystalline Holmium and Yttrium Manganite

Nor Hapishah Abdullah, Raba'ah Syahidah Azis, Muhammad Syazwan Mustaffa, Mohd Nizar Hamidon and Farah Nabilah Shafiee

Abstract

The parallel evolution of microstructure development via grain size changes from a nano-to-micron size regime toward multiferroic property development has been established in this research work. This kind of observation is not present in the literature in this research area, and studies of the link between morphological properties and ferroelectric properties of multiferroic materials have been focusing solely on the product of the ultimate sintering temperature, mostly neglecting the parallel evolutions of morphological properties and their relationship at varied chosen sintering temperatures. Holmium manganese oxide and yttrium manganese oxide were both prepared via high-energy ball milling (HEBM) in a hardened steel vial for 12 h. The pressed pellet went through multi-sample sintering, whereas the samples were sintered starting from 600 to 1250°C with 50°C increments for any one sample being subjected to only one sintering temperature. Orthorhombic $HoMn_2O_5$ and YMn_2O_5 phases were observed to exist in both as milled powder. The degree of crystallinity increased with increasing sintering temperature. Hexagonal $HoMnO_3$ peaks were observed for sintering temperature ≥1050°C. As for $YMnO_3$ series, the single phase of hexagonal $YMnO_3$ started to appear at sintering temperature ≥1000°C. FESEM micrographs revealed that as the sintering temperature increased, the grain size increased, consequently increasing the geometric ferroelectric behavior. The polarization-electric field (*P-E*) plot reveals that $HoMnO_3$ and $YMnO_3$ are highly leaky ferroelectrics with a *P-E* curve shape different from the normal shape of highly insulating ferroelectrics. It shows that the remanent polarization and electric field increased generally with increasing grain size. For both series, there existed a difference based on their difference of crystallinity, microstructure data, and phase purity changes. Larger grain size is known to give ease for polarization to take place.

Keywords: multiferroic, microstructure, holmium manganite (HMO), yttrium manganite (YMO), sintering temperature

1. Introduction of hexagonal manganites as multiferroic materials

Multiferroic materials consist of more than one ferroic polarization, and the term multiferroic was first coined by Schmid in 1994 to indicate a material that has either two or three different kinds of ferroic orders like ferromagnetism, ferroelectricity, ferroelasticity, and ferrotoroidicity in the same phase [1]. The definition is often extended to antiferroic orderings. Ferroic materials are defined as possessing a spontaneous order, the direction of which can be switched by using an external field. A ferromagnet has a spontaneous magnetization M and shows hysteresis under an applied magnetic field H. A ferroelectric has a spontaneous polarization P and shows hysteresis under an applied electric field E. As for ferroelastic, it has a spontaneous strain and shows hysteresis under an applied stress. Such spontaneous order typically occurs as a result of a phase transition when the material is cooled below a particular temperature. Following Schmid in 1994, these kinds of materials are recognized as multiferroics (**Figure 1**). Nowadays, what most people mean by multiferroic predominantly applies to the coexistence of magnetism and ferroelectricity.

In the past 5 years, research into multiferroics has branched into several different areas. The use of multiferroics for technology is currently a widely researched field, and the fundamental physics governing the strong magnetoelectric coupling seen in multiferroics is still not fully understood. Now that the causes of multiferroic behavior are better understood, it has been possible for us to observe the evolution of their microstructure with respect to their ferroelectric behavior acting in the nanoscale-to-micron-sized grain regimes. As for the chosen materials, the hexagonal rare-earth manganites, $RMnO_3$, were first discovered in 1963 [2–4]. Hexagonal $RMnO_3$ compounds show a strong ferroelectric ordering with saturated polarization larger than 5.6 μCcm^{-2} [5–7]. Thus, hexagonal rare-earth manganites are classified as an interesting family with multiferroic properties, which is also the driving force for them to be the focus of this study.

Bertaut et al. in 1963 discovered the ferroelectricity in hexagonal $REMnO_3$ [3, 4]. Precise structural investigations have been employed to find the origin of ferroelectricity in hexagonal rare-earth manganites since its discovery by Bertaut et al. [8–11]. Consequently, the origin of ferroelectricity is geometrically driven by the displacement between RE^{3+} and O^{2-} resulting from a structural phase transition. A structural phase transition from a high-temperature paraelectric phase (space group $P6_3/mmc$) to a low-temperature ferroelectric phase (space group $P6_3cm$) has been observed in hexagonal $REMnO_3$. $YMnO_3$ may serve as a representative of all hexagonal rare-earth manganite systems, especially for $HoMnO_3$ with its similar size of the rare-earth ion and lattice parameters.

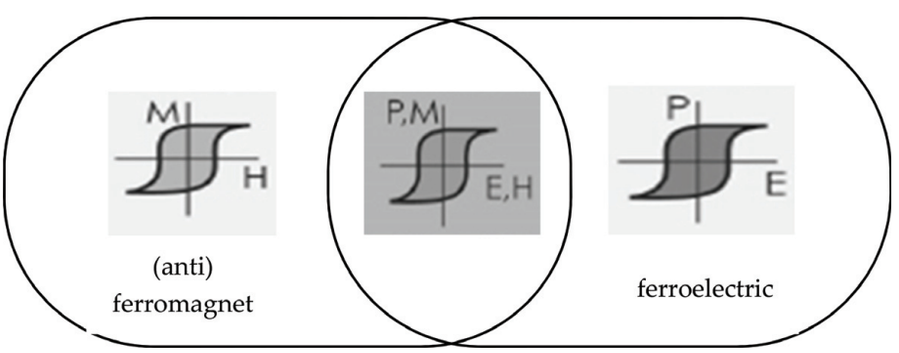

Figure 1.
Multiferroics combine the properties of ferroelectrics and magnets.

2. Brief overview of the synthesis method

Polycrystalline holmium and yttrium manganite samples were synthesized by a solid state reaction via high-energy ball milling (HEBM) with 12 h milling time. This was carried out by mixing and milling together according to the stoichiometric ratios of the required metal oxide powders, followed by pelletizing and furnace heating. The most important measurements involved in this project are ferroelectric parameters with the evolution of their microstructure. These are, ferroelectric hysteresis *P-E* loop along with microstructure analysis by FESEM measurement. For the purpose of the multiferroic material preparation in this project, the following starting materials were used:

- Holmium oxide (Ho_2O_3), 99.99%, Strem Chemicals
- Yttrium oxide (Y_2O_3), 99.99%, Alfa Aesar
- Manganese (III) oxide (Mn_2O_3), 99%, Strem Chemicals

The chemical equation via mechanical alloying (high-energy ball milling) for both desired samples are shown below:

- $0.5\ Ho_2O_3 + 0.5\ Mn_2O_3 \rightarrow HoMnO_3$
- $0.5\ Y_2O_3 + 0.5\ Mn_2O_3 \rightarrow YMnO_3$

The requirement for the sample preparation is to have the powder materials in the form of nanosized starting particles. With the use of HEBM, the duration of milling time has been chosen to be 12 h, which is optimum in order to obtain nanosized particles. The mixed material was crushed by using high-energy ball milling (HEBM) in order to facilitate the solid state reaction. The mechanical alloying (MA) process starts with mixing the powders in the right proportion and loading them into the mill along with the grinding medium (usually steel balls). The mixture is then milled for the desired length of time until a steady state is reached when the composition of every powder sample contains the same proportion of the elements in the starting powder mix. The milled powder is then transformed into a bulk shape and heat-treated to obtain the desired microstructure and properties. The key of the process involved is the raw materials, the mill, and the process variables [12]. The selected optimum parameters for the milling and ball-to-powder ratio (BPR) were 12 h and 10:1, respectively, and were used for the preparation of all the multiferroic nanoparticles used in this project. For pellet preparation, ~1.0 g is required from the as-milled powder for each sintering temperature. The mechanically alloyed nanoparticle materials were weighed according to the calculated formula using an analytical microbalance (A&D, model GR-200) and granulated by using 2% PVA. The samples were then lubricated with zinc stearate in order to reduce the density gradient caused by friction of the powder along the wall of the mold. The transformation of the previously granulated powder into a pellet shape was carried out by pressing the mold with a force of 200 MPa by using a pressing machine. Suitable pressure is important in order to obtain a uniform density compact resulting in more uniform shrinkage during sintering.

Sintering is a heating process in which the atomic mobility of the compact is sufficient to permit the decrease of the free energy associated with the grain boundaries [13]. It is the most critical and expensive process step as it yields the required crystal structure, oxidation state, microstructure, and physical condition

of a material. The purpose of the sintering process is to complete the interdiffusion of the component metal ions into the desired crystal lattices and to develop the polycrystalline microstructure at as low a temperature as possible, first to ensure a high grade of microstructural homogeneity, second to avoid cannibal grain growth, and third to save energy cost. At this stage, atoms are closely in contact with each other, hence reducing the space between them. Therefore, shrinkage occurs as a consequence of aggregation of the entire substance. As required by commercial production practice, the desired shrinkage is between 10 and 20%.

Since the aim of this research is to study in detail the evolution of the microstructure and the subsequent effect of the ferroelectric processes, sintering was used as an agent to control such desired changes that would be observed in the microstructure. The sintering temperature used for the purpose of detecting the sintering effects on the *P-E* hysteresis loops was from 600 to 1250°C with the increase of 50°C giving a total of 14 samples for each batch. They were sintered separately for 10 h in an electric furnace. The average dimensions of the final product with the pellet shape were about 10 mm diameter and 1–2 mm thickness.

3. Grain size evolution and multiferroic properties of holmium and yttrium manganite

Figure 2(a) and **(b)** shows the micrograph of the holmium and yttrium manganite powder samples milled for 12 h, which have been measured by using transmission electron microscopy (TEM) for particle size confirmation. The particle size was measured by taking diameters of 200 particles, and it was found to have inhomogeneity variation from 7 to 70 nm with an average around 27 nm (a) and 11–87 nm with average particle sizes around 30 nm (b) for holmium and yttrium manganite, respectively. The wide range of particle size distribution was due to the nonuniformity of the force between the balls and the vial during the milling process. In order to obtain a uniform grain size, particle size is an important quantity that needs to be considered. The agglomerations of the particles also occurred due to the large surface area and being subjected to repeated cold welding and fracturing during the HEBM process. This particle size is an average value considering that the particles are spherical. The particles are known to have higher reactivity due to the larger surface area. The surface atoms are more unstable (and reactive). This instability is related to their position on the lattice that forces them to unbind to their neighboring atoms or molecules. For the case of nanoparticles, as the ratio of surface/bulk atoms increases, the instability (and reactivity) also increases. Higher

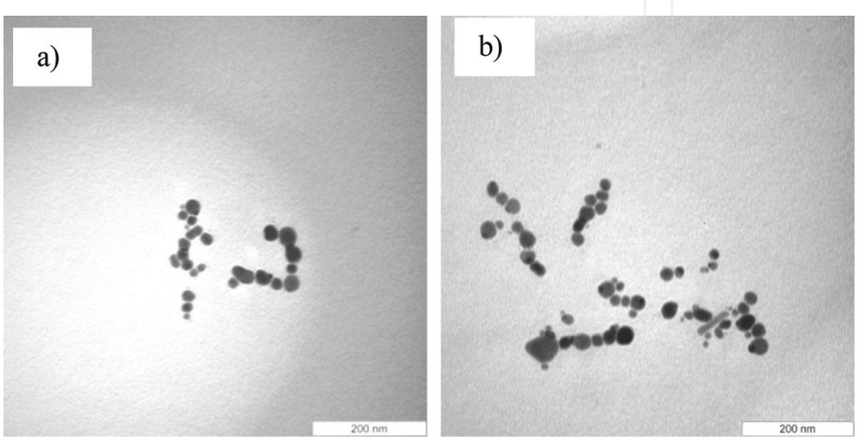

Figure 2.
TEM micrograph of resulting particles after 12 h of milling time for (a) HMO (b) YMO.

reactivity in the starting powder is required in order to prepare a series of samples in which the observation of nanosized starting particles followed by nano-to-micron size grains is required in this study.

A control of the crystal orientation is significantly important, because the ferroelectric polarization of $HoMnO_3$ and $YMnO_3$ appears along the hexagonal *c*-axis. **Figure 3(a)** and **(b)** reveals the XRD spectra of HMO and YMO samples, respectively. At 12 h high-energy ball milling, broad diffraction peaks belonging to

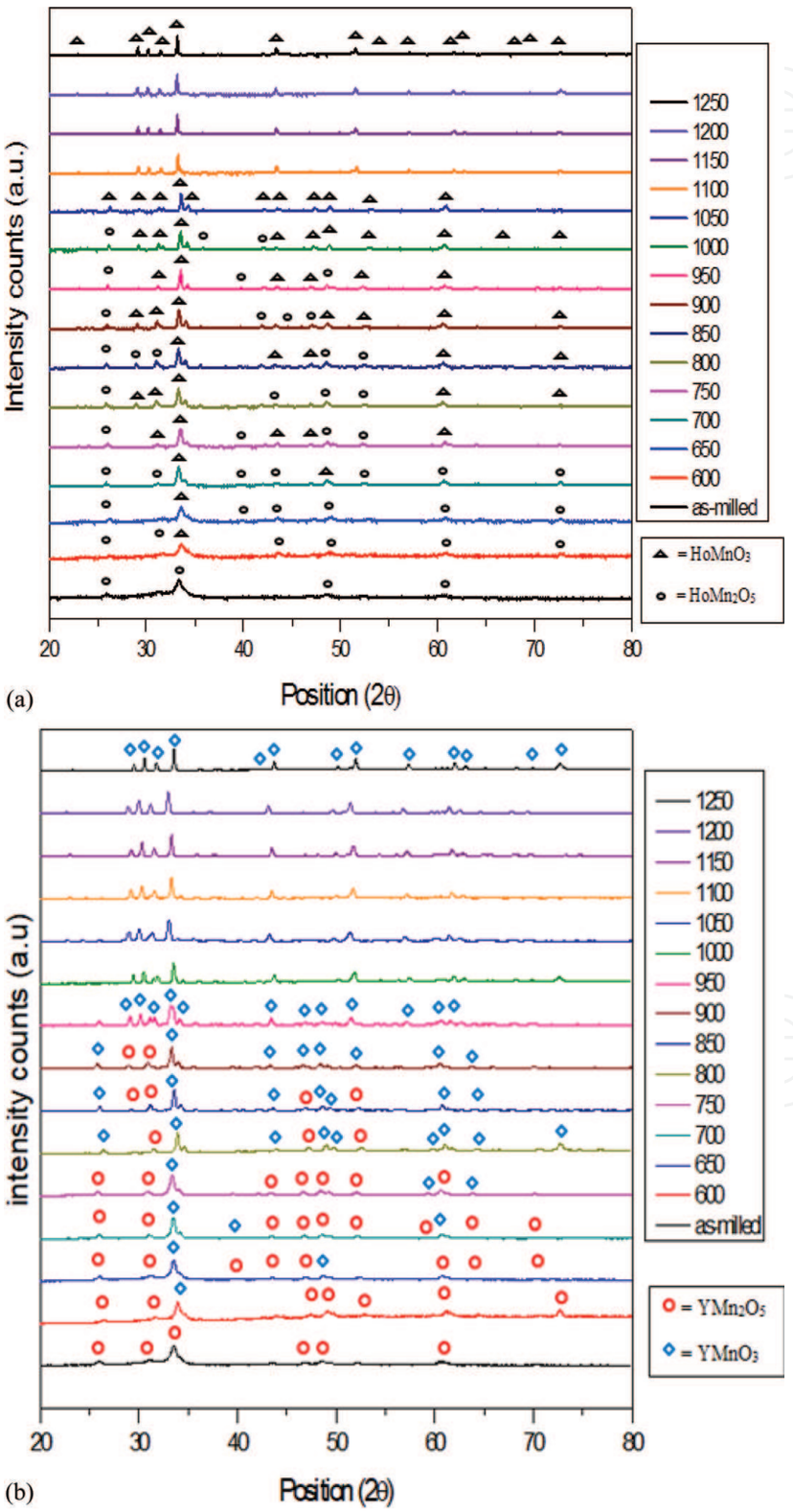

Figure 3.
(a) XRD patterns of for as milled continued with sintering from 600 to 1250°C for HMO. (b) XRD patterns of for as milled continued with sintering from 600 to 1250°C for YMO.

orthorhombic $HoMn_2O_5$ and YMn_2O_5 were observed to exist, which means that fully amorphous powders were formed. Hexagonal $HoMnO_3$ and $YMnO_3$ peaks were not observed in the as-milled powder due to insufficient thermal energy to form the structure. Impurity phases other than raw powders were not detected in the as-prepared sample. However, high-energy ball milling facilitates the reaction between the raw materials where the sintering temperature could be reduced to lower than that normally required in the conventional method due to higher surface reactivity [14]. The energy is transferred from the milling media to the powder particles by the continuous fracture and cold welding process. As the grain size started to increase, small peaks of hexagonal $HoMnO_3$ and $YMnO_3$ were detected even with fairly low intensity. Starting from 600°C sintering temperature up to 1000°C, both peaks consisting of orthorhombic $HoMn_2O_5$/ YMn_2O_5 and hexagonal $HoMnO_3$/$YMnO_3$ intensity were observed to decrease and increase, respectively. As the sintering temperature continued to increase, the secondary phase reduced in intensity. As can be seen in the figure, the main peak in each sintering temperature from 600 to 1000°C exists a splitting which is the evidence of the formation of a new structure from orthorhombic to hexagonal. The transformation from orthorhombic to a single-phase hexagonal structure started to occur at 1050°C for the HMO sample and at 1000°C for the YMO sample. Further increasing the sintering temperature from 1050 to 1250°C raised the intensity of the major peaks belonging to hexagonal holmium and yttrium manganese oxide ($HoMnO_3$ and $YMnO_3$), which demonstrated the improvement in the degree of crystallinity of the sintered samples besides releasing the strain induced by milling. The results demonstrate that the hexagonal phase of $HoMnO_3$ and $YMnO_3$ could not be formed only by milling since the energy imparted by the collision of the milling media to the starting powders is not sufficient to increase the reactivity between the particles. Besides, without the sintering process, insufficient energy will be provided to stimulate the reaction between particles. As the sintering temperature increases, a larger grain size would be formed due to the combination of grains, thus inducing the formation of a more crystalline phase with a hexagonal structure. Furthermore, a ferroelectric phase would be formed because of the increasing electric dipole moment of the crystalline hexagonal structure, whereas it is known that ferroelectricity is geometrically driven by the displacement between RE^{3+} and O^{2-} as a result of a structural phase transition [8–11]. Therefore, a higher sintering temperature, say 1250°C, would lead to a higher value of dielectric constant and ferroelectric order. At lower sintering temperature, the sample exhibited a smaller grain size that will contribute a larger amount of amorphous grains compared to samples with a larger grain size. This amount was significant in view of the fact that the grain boundary volume was not negligible for the nanometer grain size [15].

The microstructural images of the sintered pellets were obtained using a Nova NanoSEM 50 scanning electron microscope. The SEM micrographs of the HMO and YMO samples are shown in **Figures 4(a)–(n)** and **5(a)–(n)**. In the HMO samples, the sintering temperature from 600 to 900°C with a grain size of 30 to 65 nm determines the slow rate of grain growth, while at 950, 1000, and 1050°C (from 108 to 296 nm), it indicates moderate increment. The grain growth was observed to be increased at 1100 up to 1250°C (854 nm–2.9 μm) due to creation of a pure single hexagonal HMO phase. As for the YMO samples, grain growth occurred at 600–900°C (from 49 to 75 nm) and continued by adequate increment at 950, 1000, and 1050°C (from 82 to 314 nm). The grain growth was observed to be increased at 1100°C up to 1250°C (543 nm–2.1 μm). The results demonstrate that multi-sample sintering involved a transition from the slow-moderate-rapid grain growth process. The grains grew at the expense of others and were created from movement of grain boundaries and grains, respectively. The pores will form an interconnected channel along grain edges when

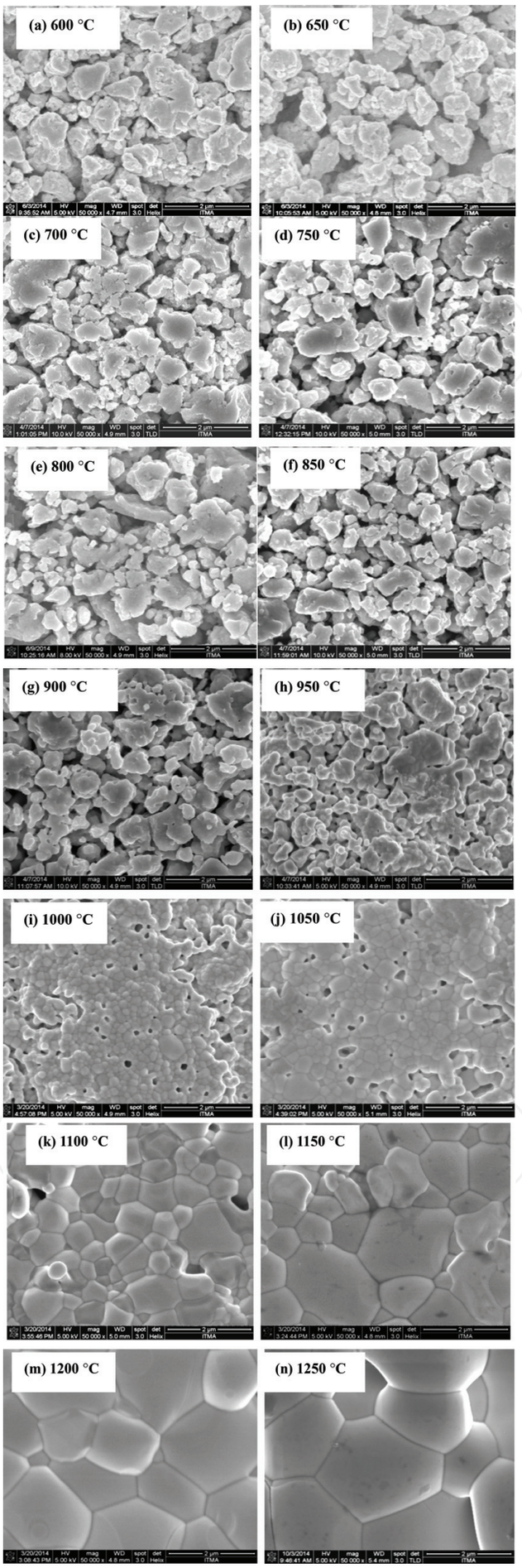

Figure 4.
(a–n) FESEM micrograph from 600 to 1250°C for HMO.

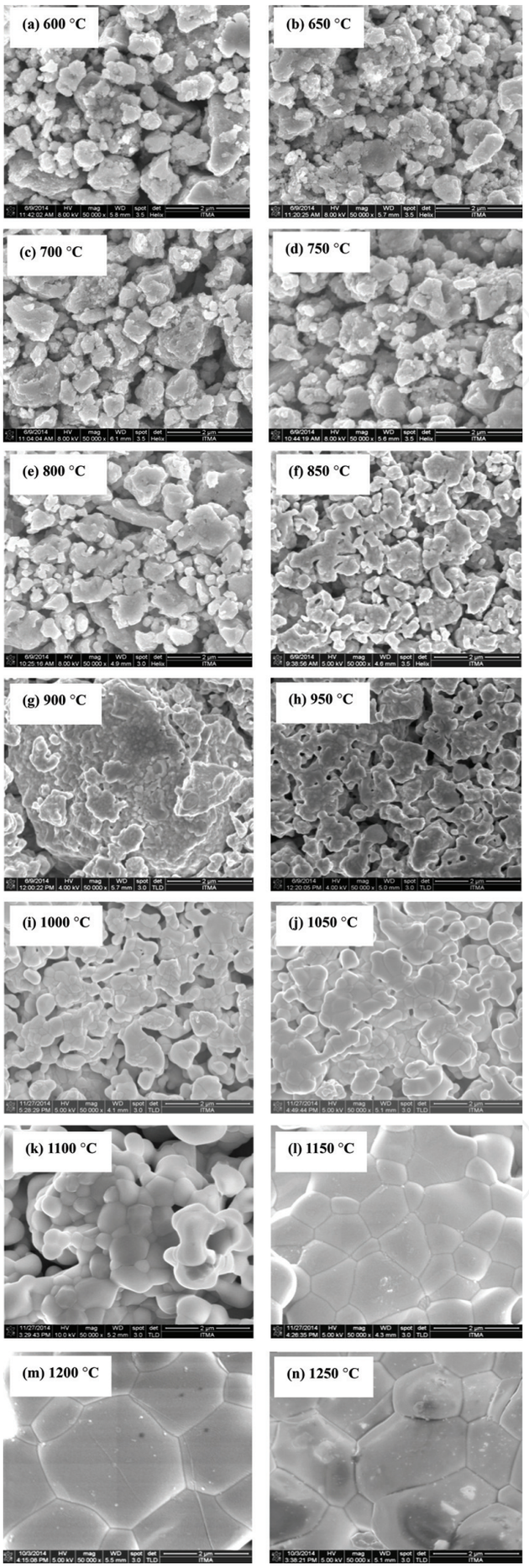

Figure 5.
(a–n) FESEM micrograph of YMO sintered from 600 to 1250°C.

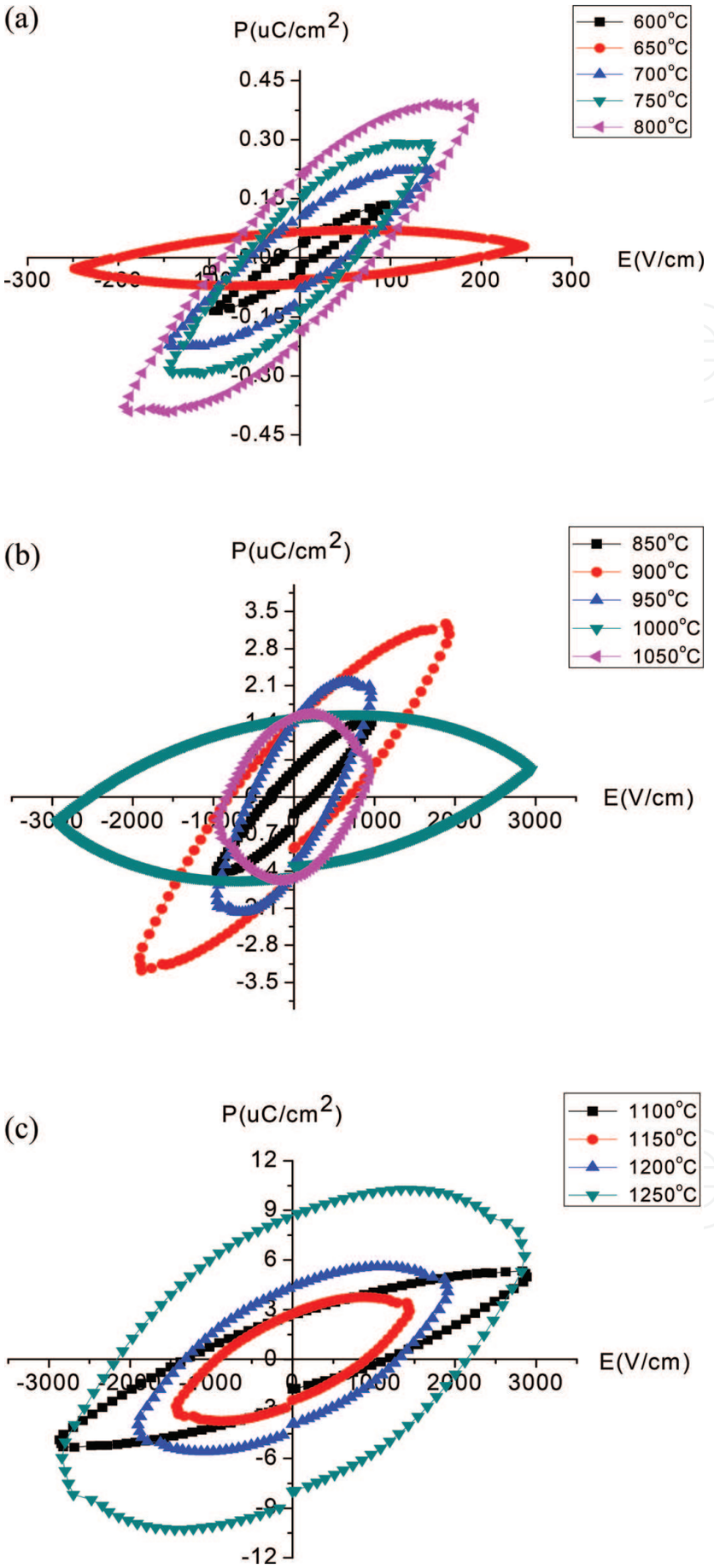

Figure 6.
(a) P-E for HMO samples sintered at 600–800°C. (b) P-E for HMO samples sintered at 850–1050°C. (c) P-E for HMO samples sintered at 1100–1250°C.

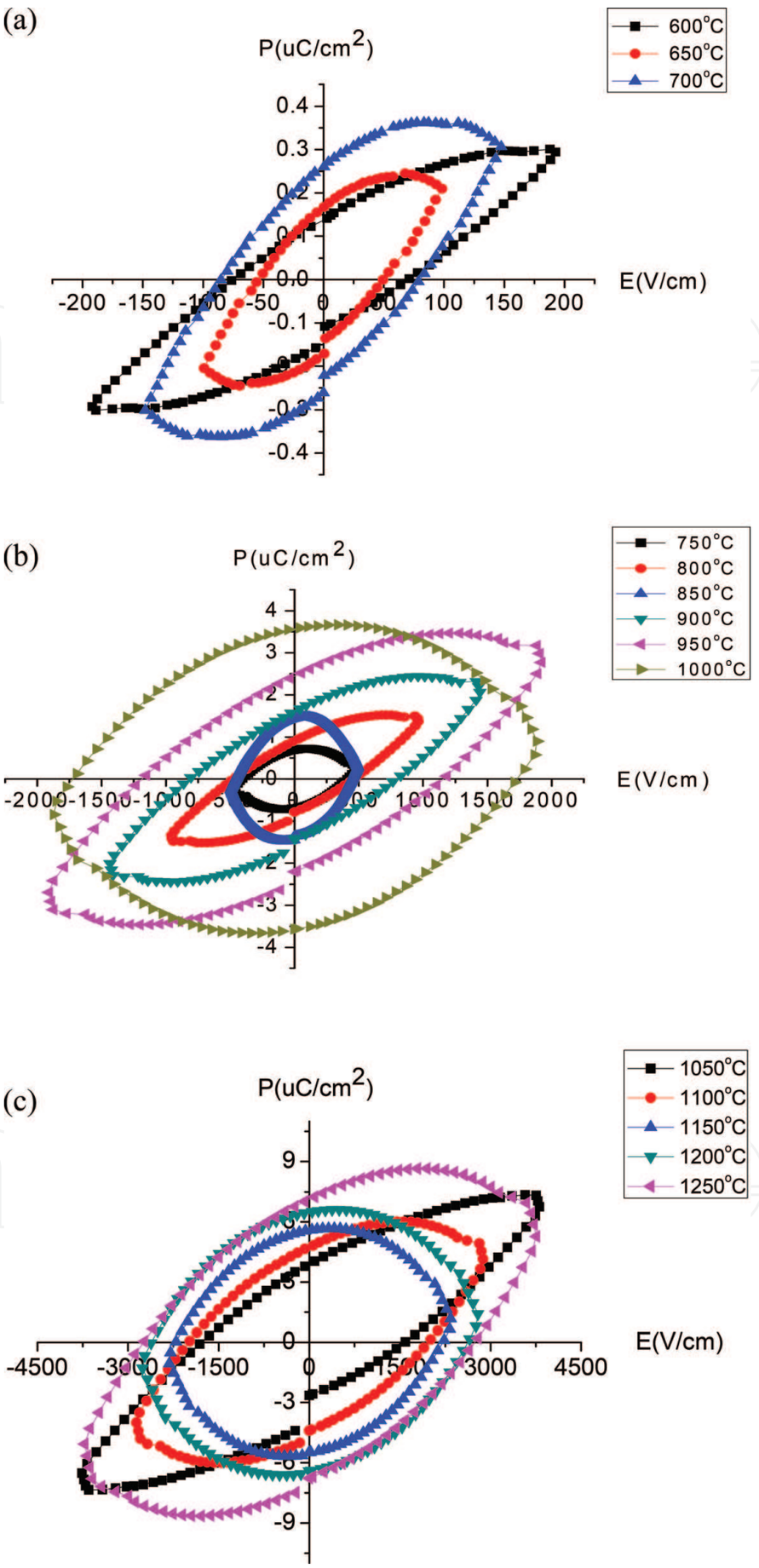

Figure 7.
(a) P-E for YMO samples sintered at 600–700°C. (b) P-E for YMO samples sintered at 750–1000°C. (c) P-E for YMO samples sintered at 1050–1250°C

there is formation of a necking process between particles in the powder compacts. However, the pore channels were disconnected and isolated when the sintering process was introduced. Microstructural interpretations at higher sintering temperatures from 1100 to 1250°C in **Figures 4(k)–(n)** and **5(k)–(n)** correspond to the final stage of sintering. The diffusion process of vacancies from the pores along grain boundaries will cause the pores grew to be closed and have been slowly eradicated with a slight densification. The grains with a hexagonal structure could be perceived in this stage as the sintering temperature and grain size increased.

Figures 6(a)–(c) and **7(a)–(c)** show the polarization induced by applying an electric field for all sintered samples of HMO and YMO, respectively. Lower sintering temperatures, 600–800°C for the HMO *PE* loop (**Figure 6a**) and 600–700°C for YMO (**Figure 7a**), reveal a lossy capacitor response with low P_r, indicating the major paraelectric behavior contributed by a large amount of orthorhombic phase with very little contribution of the hexagonal phase. It is speculated that the presence of the second phase (shown in the XRD spectra) makes the electron to be detached and free as free charges which contributed to cause the loop to leak. As the sintering temperature increased from 850 to 1050°C for HMO (**Figure 6b**) and 750 to 1000° C for YMO (**Figure 7b**), an ideal resistor response curve with higher values of P_r and E_c was obtained. This is due to the existence of the geometric ferroelectric derived from the hexagonal phase, which started to dominate as the grain size increased with the increase of sintering temperature. The grain boundary volume in a smaller grain size is higher compared to a larger grain size, which was the reason why the P_r got better as the grain size increased. The effect of grain boundary on polarization includes two factors. The first one is, the grain boundary is a low-permittivity region, which means that the grain boundary has poor ferroelectricity with little or even no polarization. Secondly, space charges in the grain boundary exclude polarization charge on the grain surface, which would form a depletion layer on the grain surface, which results in polarization discontinuity on the grain surface to form a depolarization field and the polarization decreases. At higher sintering temperature as seen in **Figure 6c** for HMO and **Figure 7c** for YMO, it was confirmed that the contribution of the majority hexagonal phase has improved the geometric ferroelectric behavior. Sintering at higher temperature shows the increase of the average grain size, which gave a good response in the polarization hysteresis loop. The contribution of larger grains reduced the secondary peaks while having high crystallinity and enhancing the response of the electric field. As shown in the polarization hysteresis (**Figures 6** and 7), applying the electric field increases the polarization values but still showed that the *P-E* hysteresis loops are not saturated. HMO and YMO are known to behave as a leaky ferroelectric as mentioned in previous reports [16, 17]. As can be seen in **Figures 6** and 7, the shapes of the hysteresis loop are mainly related to the combination of an ideal resistor and lossy capacitor response. The mobility of free charges will also contribute to higher conductivity and cause higher leaking current, which would be the main reasons for the E_c values to be unpredictable. Even though the hysteresis loops are seen to be leaky in nature, they are still significant enough to definitely confirm the ferroelectricity of the HMO and YMO samples.

4. Conclusion

$HoMnO_3$ and $YMnO_3$ multiferroics were successfully synthesized via high-energy ball milling, and the parallel evolution of ferroelectric with microstructural properties has been studied. High-energy ball milling was able to produce high-

degree crystallinity and some trends of electrical properties due to the high surface reactivity of starting materials. It must be noted that this clear understanding has been made possible only through a progressive sintering scheme of nanometer-particle compacts from an unusually low sintering temperature (600°C) to a somewhat high sintering temperature (1250°C). From the discussion presented, the evolution of a nanometer-to-micron grain size regime has been presented and the changing patterns of ferroelectrics are now clearly understood. It was found that the ferroelectric and magnetic properties generally correlated with intrinsic and extrinsic properties. The intrinsic contribution came from the contribution of the crystal structure in which orthorhombic, hexagonal, and more or less orthorhombic + hexagonal phases affected the phase that will contribute to the proper behavior of the ferroelectric. The effects of grain size of the two series of manganites have been observed by the scheme of nanosized starting particles followed by nano-to-micron grain sized regime data. Microstructural changes revealed a revolution of the crystal structure from orthorhombic to hexagonal at a larger grain size regime. The ferroelectric behavior was also observed to change with the change of microstructure along with the structural transformation from orthorhombic to hexagonal. For a general conclusion, the intrinsic effect occurred in the low sintering temperature region (600–1000°C for $HoMnO_3$) and (600–900°C for $YMnO_3$). The property changes at this region are due to crystal structure transformation. The extrinsic effect was more obvious at higher sintering temperature that is 1050–1250°C for $HoMnO_3$ and 950–1250°C for $YMnO_3$ in the hexagonal structure. The optimum condition to obtain a sample with very fine properties could be obtained by performing high-energy ball milling for 12 h followed by sintering at 1250°C with 10 h holding time. These steps were required in order to reach a very stable hexagonal structure for most advantageous ferroelectric and magnetic properties. The study of the evolution work has resulted in greater appreciation of the theoretical and experimental difficulties involved, if not in new knowledge of the behavior of multiferroic studies in evolution. In fact, there were no reported studies regarding these evolution works in the multiferroic field.

Acknowledgements

The authors are thankful to the Materials Synthesis and Characterization Laboratory (MSCL), Functional Devices Laboratory (FDL), Institute of Advanced Technology (ITMA), and also the Department of Physics, Faculty of Science, Universiti Putra Malaysia (UPM), for the measurement facilities.

DOI: http://dx.doi.org/10.5772/intechopen.81753

IntechOpen

Author details

Nor Hapishah Abdullah[1], Raba'ah Syahidah Azis[2,3]*,
Muhammad Syazwan Mustaffa[2], Mohd Nizar Hamidon[1] and Farah Nabilah Shafiee[3]

1 Functional Devices Laboratory (FDL), Institute of Advanced Technology, Universiti Putra Malaysia, UPM, Serdang, Selangor, Malaysia

2 Department of Physics, Faculty of Science, Universiti Putra Malaysia, UPM, Serdang, Selangor, Malaysia

3 Materials Synthesis and Characterization Laboratory (MSCL), Institute of Advanced Technology, Universiti Putra Malaysia, UPM, Serdang, Selangor, Malaysia

*Address all correspondence to: rabaah@upm.edu.my

IntechOpen

© 2019 The Author(s). Licensee IntechOpen. This chapter is distributed under the terms of the Creative Commons Attribution License (http://creativecommons.org/licenses/by/3.0), which permits unrestricted use, distribution, and reproduction in any medium, provided the original work is properly cited. CC BY

References

[1] Schmid H. Multiferroic magnetoelectrics. Ferroelectrics. 1994; **162**:317-338

[2] Subba Rao GV, Chandrashekhar GV, Rao CNR. Are rare earth orthochromites ferroelectric?. Solid State Communications. 1968;**6**(3):177-179

[3] Kovalev AV, Andreeva GT. Low temperature X-ray study of $Ni_3B_7O_{13}I$ boracite. Comptes Rendus Academy of Science. 1956;**2**:56

[4] Coeure P, Guinet F, Peuzin JC, Buisson G, Bertaut EF. Ferroelectric properties of hexagonal orthomanganites of yttrium and rare earths. Proceeding International Meeting Ferroelectric (Prague). 1966;**1**: 332

[5] Katsufuji T, Mori S, Masaki M, Moritomo Y, Yamamoto N, Takagi H. Dielectric and magnetic anomalies and spin frustration in hexagonal $RMnO_3$ (R=Y, Yb, and Lu). Physical Review B. 2001;**64**:1-6

[6] Lottermoser T, Lonkai T, Amann U, Hohlwein D, Ihringer J, Fiebig M. Magnetic phase control by an electric field. Nature. 2004;**430**:541-544

[7] Fiebig M, Lottermoser T, Fröhlich D, Goltsev AV, Pisarev RV. Observation of coupled magnetic and electric domains. Nature. 2002;**419**:818-820

[8] Yakel HL, Koehler WD, Bertaut EF, Forrat F. On the crystal structure of the manganese (III) trioxides of the heavy lanthanides and yttrium. Acta Cryst. 1963;**16**:957

[9] Aken BBV, Bos JWG, Groot RA, Palstra TTM. Asymmetry of electron and hole doping in $YMnO_3$. Physical Review B. 2001;**63**:125-127

[10] Aken BBV, Palstra TTM, Filippetti A, Spaldin NA. The origin of ferroelectricity in magnetoelectric $YMnO_3$. Nature Materials. 2004;**3**: 164-170

[11] N'enert G. Orbital ordering and multiferroics [PhD thesis]. The Netherlands: University of Groningen. Vol. 55–59; 2007. pp. 93-96

[12] Suryanarayana C. Mechanical alloying and milling. Progress in Materials Science. 2001;**46**:1-184

[13] Slick PI. Ferromagnetic Materials. Vol. 2. The Netherlands: North-Holland Publishing Company; 1980. p. 209

[14] Waje SB, Hashim M, WanYusoff WD, Abbas Z. Sintering temperature dependence of room temperature magnetic and dielectric properties of $Co_{0.5}Zn_{0.5}Fe_2O_4$ prepared using mechanically alloyed nanoparticles. Journal of Magnetism and Magnetic Materials. 2010;**322**:686-691

[15] Idza IR, Hashim M, Rodziah N, Ismayadi I, Norailiana AR. Influence of evolving microstructure on magnetic-hysteresis characteristics in polycrystalline nickel-zinc ferrite, $Ni_{0.3}Zn_{0.7}Fe_2O_4$. Materials Research Bulletin. 2012;**47**:1345-1352

[16] Sahu JR, Ghosh A, Rao CNR. Multiferroic properties of $ErMnO_3$. Materials Research Bulletin. 2009;**44**: 2123-2126

[17] Scott JF. Ferroelectric go bananas. Journal of Physics: Condensed Matter. 2008;**20**(2):1-2